CELLULAR IMMUNOLOGY 15, 109–128 (1975)

Thymus Cell Maturation

II. Differentiation of Three "Mature" Subclasses *in Vivo*[1]

C. GARRISON FATHMAN,[2] MYRA SMALL,[3] LEONARD A. HERZENBERG,[4] AND IRVING L. WEISSMAN[5,6]

Laboratory of Experimental Oncology, Department of Pathology, and Department of Genetics, Stanford University School of Medicine, Stanford, California 94305

Received May 7, 1974

Several thymus cell subclasses may be defined on the basis of their sedimentation velocity, their light-scattering properties (a measure of cell volume), or binding of a fluoresceinated anti-Thy 1.2 antiserum. Using a multiparameter fluorescence-activated cell sorter (FACS), cells with distinguishable light-scattering or fluorescence intensity (after staining with fluorescein anti-Thy 1.2) were separable for analysis of intrathymic maturation pathways. Outer thymic cortical large and medium lymphocytes were the only cells labeled within 1 hr after transcapsular diffusion of administered [^{3}H]thymidine. These labeled cells were also entirely contained in the brightest fluorescence intensity (with fluorescein anti-Thy 1.2) subclass. Under conditions of [^{3}H]thymidine "chase" *in vivo*, label shifted proportionately and apparently in parallel to three "mature" subclasses: (1) small thymocytes with high surface concentrations of Thy 1.2, representing $\sim$ 80% of all thymus cells; (2) slightly larger cells, with very low surface Thy 1.2, which are indistinguishable from cortisone-resistant thymocytes, and which make up less than 10% of all thymus cells; (3) dead or fragile cells.

INTRODUCTION

Cellular differentiation in the thymus presumably leads to the development of immunocompetent peripheral "T" lymphocytes. Although the process by which these cells are generated from immunoincompetent thymic precursors has not yet been elucidated, there are considerable data showing the existence of a small pool of immunocompetent cortisone-resistant, medullary thymocytes which, as a population, bear low concentration of Thy 1.2,[7] lack TL antigens, and exhibit high

[1] Supported by USPHS Grants AI-09072 and GM-17367.

[2] Present address, National Cancer Institute, Bethesda, MD 20014.

[3] Stanley McCormick Fellow; present address: Department of Cell Biology, Weizmann Institute for Science, Rehovoth, Israel.

[4] Department of Genetics.

[5] Senior Dernham Fellow in Oncology, California Division, American Cancer Society.

[6] To whom reprint requests (and correspondence) should be sent.

[7] Abbreviations: ^{3}HTdR, tritiated thymidine; α, anti; Thy 1.2, ΘC3H alloantigen; FACS, fluorescence-activated cell sorter; CSM, cell-suspending medium; FBS, fetal bovine serum; rpm, revolutions per minute; FITC, fluorescein isothiocynate; F/P, moles fluorescein bound per mole protein; CR, cortisone-resistant cells remaining in the thymus 2 days after parenteral injection of hydrocortisone acetate; CS, cortisone-sensitive cells; NT, normal thymocytes (from an untreated donor); PHA, phytohemagglutinin; Con A, Concanavalin A.

concentrations of H-2. Two possible maturation sequences exist: Immunocompetent subpopulations may be derived from immunoincompetent precursors or may be derived from a self-generating pool of cells independent from the immunoincompetent pool. However, at least some of the cortisone-resistant medullary thymocytes are derived from an intrathymic pool of cortisone-sensitive cortical precursors (1).

The process of thymic cell maturation can be followed by topical application of radioactive nucleosides to the thymus, resulting initially in labeling of larger thymocytes in the outer thymic cortex (1, 2). These cells give rise to smaller, nondividing thymic lymphocytes. The observation of this size progression during the course of maturation, as well as the existence of subpopulations of cells with apparently low and high surface levels of Thy 1.2 suggested that separation techniques based on cell size or Thy 1.2 expression might aid in delineating the details of the maturational process. In this paper we describe studies of thymocyte subpopulations and their intrathymic maturational patterns after thymus topical [^{3}H]-thymidine labeling. The methods employed are 1g sedimentation and, using a fluoresence-activated cell sorter (FACS), low-angle light scatter (an independent volume measurement), and quantitative anti-thy 1.2 fluorescence measurements of individual cells.

MATERIALS AND METHODS

Young postnatal (4- to 8-day) and 4-wk-old male BALB/c mice were used in all experiments. Their thymocytes were labeled *in vivo* with [^{3}H]thymidine (New England Nuclear, Boston, MA) and suspended *in vitro* as described previously (1). In a few experiments, *in vitro* labeling of thymocytes with ^{51}Cr (New England Nuclear, Boston, MA) was accomplished by incubation of 1×10^8 thymocytes in 1 ml of a cell-suspending medium (CSM5: Bicarbonate-buffered Medium 199 [GIBCO, Grand Island, NY] with 100 U penicillin and 100 μg streptomycin/ml and 5% heat-inactivated fetal bovine serum [FBS Microbiological Associates, Bethesda, MD]) with 150 μCi ^{51}Cr for 1 hr, followed by three washes in cold chromium-free CSM5.

In some experiments, mice were injected intramuscularly (im) with 5 mg (5-wk-old hosts) or 2.5 mg (5-day-old hosts) hydrocortisone acetate (Invenex Pharmaceuticals, San Francisco, CA) 2 days before removing thymuses for cell studies.

Unit Gravity Sedimentation of Thymocytes

Thymocyte suspensions were separated by the velocity sedimentation technique developed by Miller and Phillips (3) using a commercial STAPUT apparatus with a 180-mm diam sedimentation chamber, manufactured by Johns Scientific (Toronto, Canada). In most experiments, 2×10^8 cells introduced in 80 ml of CSM3 (3% FBS) were allowed to sediment for 12 hr at 4° C through a gradient composed of 940 ml CSM30 (30% FBS), 940 ml CSM15 (15% FBS), and 40 ml CSM5. Sixty fractions of 30 ml were collected, centrifuged for 10 min at 1500 rpm (International Centrifuge, Model PR-J, Head No. 269), resuspended in 2.5 ml CSM5, and aliquots taken for various measurements. Cell numbers per fraction were determined with a Coulter Counter (Model B, Coulter Electronics, Hialeah, FL). Estimations of cell size were made by Coulter-counter size distributions and microscopic examination of cytocentrifuge preparations (Sakura Finetechnical Ltd., distributed by Canalco, Rockville, MD). Measurement of [^{3}H]thymidine (in sedi-

mentation fractions) was performed by transferring 200-μl aliquots to a microtiter plate, centrifuging at 2200 rpm for 10 min, removing supernatant fluid, solubilizing the cell pellets in 0.1 ml 1 *N* NaOH overnight, and counting solubilized samples in scintillation fluid in a liquid scintillation counter (4). Autoradiography was performed as described previously (5). Measurement of ^{51}Cr was achieved by counting aliquots directly in a gamma spectrometer.

Fluorescence Analysis and Separation of Cells Using a Fluoresence-Activated Cell Sorter (FACS)

Description of construction and use of a FACS has been reported (6, 7). This instrument allows analysis and/or separation of $\sim 10^4$ cells/sec. Two independent parameters for each cell are measured simultaneouly on cells passing in single file in a jet stream: intensity of fluorescence and intensity of low-angle light scattering. The latter is closely correlated with cell volume for live cells and can also be used to readily distinguish dead from live lymphoid cells. Electrical pulses generated by each cell for fluorescence and scatter are accumulated and displayed by pulse-height analyzers. The pulse-height analyzers give frequency distributions of the relative scatter or fluorescence intensities per cell. These distributions are plotted with relative cell numbers displayed along the ordinate and increasing intensity of fluoresence or scatter (volume) displayed along with the abscissa.

By electronic means it is possible to display the fluoresence distribution of only those cells having a particular, preset, range of scatter intensities. Such a distribution is called a scatter-gated fluorescence profile and conveniently permits fluorescence to be electronically "noted" and recorded only of, for example, all live cells (since live and dead cells have distinctive scatter intensities) or of only the largest 20% of live cells. These various photodetection parameters may be used to impose a preset charge onto droplets (emerging from the jet stream) containing the cell which possessed the desired properties. These droplets then pass through a charge field which deflects them on the basis of the charge they possess.

Antisera Preparation

Anti-Thy 1.2 antisera were raised by weekly injections of AKR/J mice with either CBA/J or C3H/J thymocytes until high-titered complement-dependent cytotoxic antibodies to BALB/c thymocytes were obtained. All cytotoxicity and fluorescence staining activity of these sera against BALB/c thymocytes were removed by absorption with C3H or BALB/c brain, and no decrease in cytotoxicity or fluorescence was seen after absorption with 1×10^8 AKR/J thymocytes, or by addition of BALB/c serum. Anti-TL antisera were raised in C57BL/6J mice by weekly or biweekly injections ($\frac{1}{2}$ to $\frac{1}{10}$ donor per host of C57BL/6JTLa thymocytes (mice congenic except for the TLa locus, kindly provided by E. A. Boyse) for 20 injections. This antiserum cytolyses 85%–90% of C57BL/6J TLa or A/JAX thymocytes in the presence of complement. All cytotoxic tests were carried out in a two-step ^{51}Cr-release assay system, using either absorbed fresh guinea pig serum or unabsorbed horse serum (SE 174) selected for low background lysis at 1:8 as a complement source.

For fluorescence analysis, the antisera listed above were either conjugated with FITC as previously described (8), or used in a two-stage sandwich technique in

which a specific fluorescent-labeled rabbit anti-mouse IgG was added as a second step. Cells were incubated with antisera (F/P ratio of from 1 to 2) at 4° C for 30 min, at 1:10 to 1:60 dilution depending upon their relative titer (as assayed by FACS quantitative fluorescence), washed extensively, and pelleted through FBS prior to use.

Viability Staining

Viability was assayed by trypan blue exclusion and fluorescein diacetate staining (9).

Cosedimentation Analysis

Thymocytes (2×10^7) were labeled *in vitro* with ^{51}Cr, as described, and then mixed with 2×10^8 adult BALB/c thymocytes for sedimentation analysis. Fractions were collected, cell numbers recorded, and aliquots of each fraction were counted in a γ-spectrometer.

A cosedimentation index comparing test and control cell suspensions for each sedimentation fraction was derived using the following formula:

$$\text{Cosedimentation Index (CI)} = \frac{\gamma \text{ counts in test fraction}/\gamma \text{ counts in total gradient}}{\text{Cell counts in test fraction/Cell counts in total gradient}}.$$

Similarly, FACS-sorted fractions were scored for enrichment or depletion of percentage of labeled cells by the following formula:

$$\text{Cell Sorting Labeling Index (CSLI)} = \frac{\%\text{ labeled cells in test thymocyte fraction}}{\%\text{ labeled cells in unfractionated thymocyte suspension}}.$$

RESULTS

Our initial experiments were aimed at defining the size and Thy 1.2 antigenic subclasses of BALB/c thymocytes. In a later section, we identify some of the inter-subclass maturation patterns by selective labeling of a single subclass of precursor cells.

Size Distribution of Normal Thymocytes Separated by Velocity Sedimentation and the FACS

The distribution of cells obtained by 1*g* sedimentation is shown in Fig. 1a and the scatter (volume) analysis of the three indicated cell pools, A, B, and C, obtained with FACS is shown in Fig. 1b. (Total cell recovery in that experiment was 87.7% of input cell numbers.) It is apparent that the modal cell number lies in small lymphocyte region (labeled A in Fig. 1a and 1b), containing ~80% of the total recovered cell population. Fractions 1 to 32 contain large to medium cells as verified by FACS scatter analysis of two pools (B and C) from these gradient regions (Fig. 1b). Smudge cells appear in increasing numbers after fraction 45; in this experiment they consitute 7.1% of recovered cells. Morphological analysis

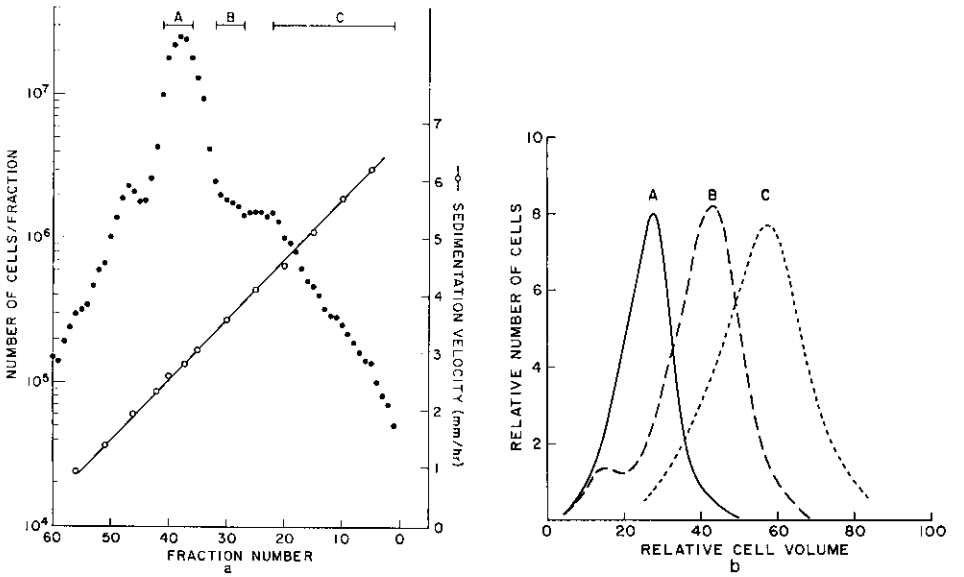

FIG. 1. a. Sedimentation profile of a 5-wk-old BALB/c donor's thymocyte suspension: 2×10^8 cells were layered over an FBS–CSM gradient as described in Materials and Methods, and allowed to sediment at 4° C for 12 hr. The ordinate is the logarithm of the number of cells per fraction, and the abscissa the fraction number. Pools A, B, and C, as indicated, were removed for scatter analysis (Fig. 1b). b. Frequency distributions of scatter signals derived by analyzing three separate pooled fractions from the 1*g* gradient. The abcissa portrays increasing cell volume, the ordinate relative numbers of cells. The height of each scatter plot is a function of the number of cells analyzed and does not indicate the number of cells per fraction. These and all subsequent scatter plots were generated in the FACS.

of cytocentrifuge preparations of sedimentation fractions reveals a continuum of cell sizes from large to small cells with increasing fraction number.

Figure 2a shows the scatter distribution of normal thymocytes. Separated peaks

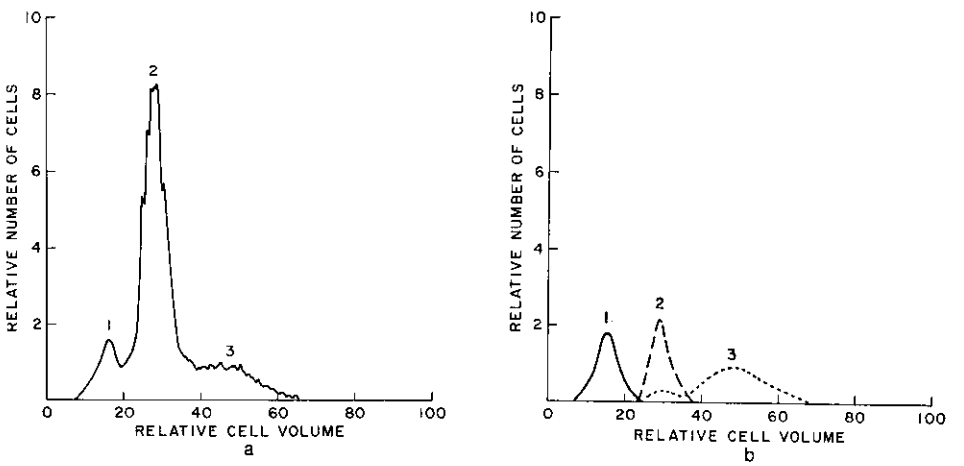

FIG. 2. a. Frequency distribution of scatter signals generated by normal thymocytes in suspension. Three separate subpopulations are observed. These are labeled 1, 2, and 3. b. Reanalysis by scatter of the three subpopulations of thymocytes separated according to scatter. These three frequency distributions show only relative cell volume per fraction and give no representation of the total cell count per fraction.

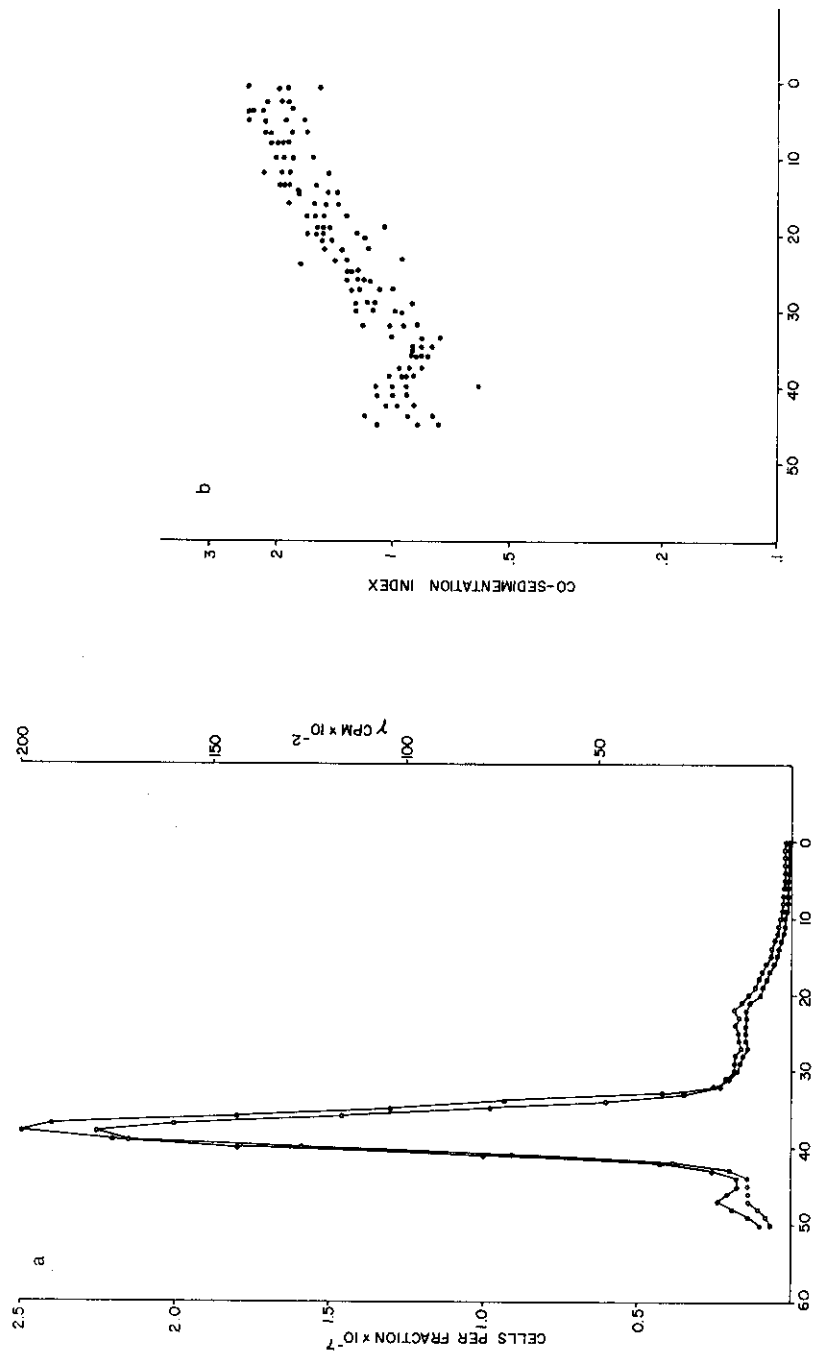

FIG. 3. Cosedimentation analysis of 5-wk-old BALB/c donor thymocytes: 2×10^7 ^{51}Cr-labeled thymocytes were cosedimented with 2×10^8 unlabeled thymocytes from the same supension and the results plotted either directly (3a), or (3b) as the logarithm of the Cosedimentation Index (see Methods) on the ordinate vs fraction number on the abcissa (four experiments plotted).

1, 2, and 3 are reanalyzed by scatter in Fig. 2b, demonstrating the reproducibility of this fractionation technique. Reported elsewhere (7) is evidence that the first peak contains predominantly dead cells. Morphologically, the scatter-separated peaks are similar to their 1*g* separated counterparts. Peak 1 consists predominantly of smudge cells—verifying that nonviable cells do indeed smudge in cytological preparations (10). Peak 2 cells are predominantly small, viable lymphocytes, whereas peak 3 contains a wide distribution of large and medium viable lymphocytes.

Sedimentation and Scatter Analysis of Cortisone-Resistant Thymocytes

Since cortisone-resistant (CR) thymocytes appear to be derived (at least in part) from cortisone-sensitive (CS) precursors, experiments were performed to determine what size categories were enriched after administration of cortisone *in vivo*. Those thymus cells remaining 48 hr after im injection of 5 mg hydrocortisone acetate in adults or 2.5 mg in 5-day-old BALB/c mice were suspended, and cosedimented as described in Materials and Methods.

As a check on the accuracy of the method, we ran seven experiments wherein 2×10^7 NT cells were labeled *in vitro* with ^{51}Cr, and then cosedimented with 2×10^8 NT cells from the same thymus. In all cases, the cell number and γ-count peaks coincided. In six of seven experiments, the relative uptake of ^{51}Cr by larger cell fractions (1–25) was greater than in the smaller cell fractions (25–56) as demonstrated in Fig. 3.

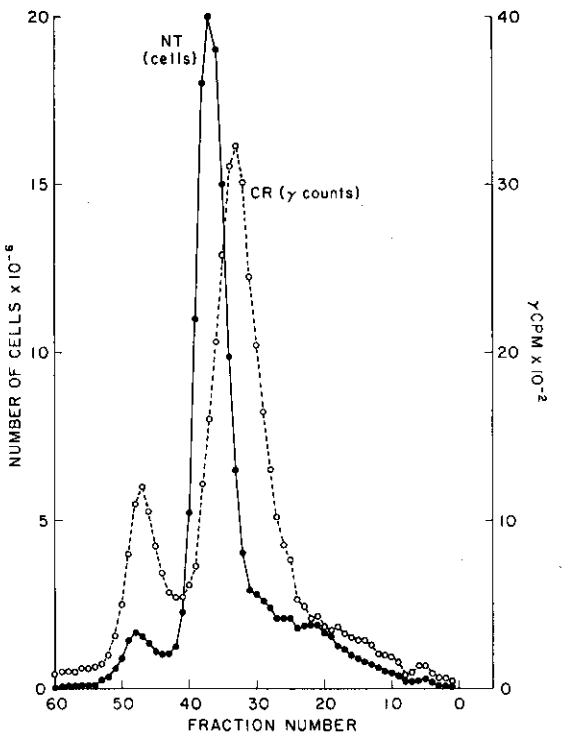

FIG. 4. Cosedimentation analysis of 5-wk-old BALB/c donor thymocytes: 2×10^7 ^{51}Cr-labeled CR thymocytes were cosedimented with 2×10^8 unlabeled thymocytes from untreated donors. On the ordinate, either ^{51}Cr or cell counts are recorded for each of the indicated fractions.

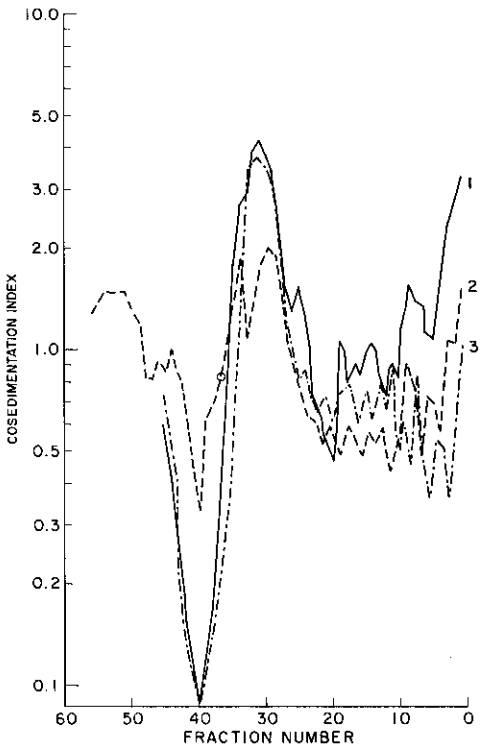

FIG. 5. Cosedimentation index profile of ^{51}Cr-labeled 5-wk-old BALB/c donor CR cells cosedimented with 5-wk-old untreated donor thymocytes. Axes as in Fig. 4.

A typical curve of cosedimented normal thymocytes (NT) and CR cells is shown in Fig. 4. It is apparent that the peak of CR cells is at a higher sedimentation velocity (fraction 34, ~ 3.1 mm/hr) than the modal peak of NT cells (fraction 37, ~ 2.8 mm/hr), although there is considerable overlap. The cosedimentation profiles of CR vs NT from adult (Fig. 5) and neonatal (Fig. 6) thymuses reveals a maximum enrichment of CR cells at fraction 30, although the peak of CR cells is usually at fraction 34. (For subsequent experiments, fractions 28–32 were chosen for the highest proportion of CR-like cells.) Scatter analyses of CR and NT cells are plotted together in Fig. 7, and appear quite similar to the cosedimentation curve shown in Fig. 4.

Thus, size analysis of BALB/c thymocytes reveals at least four distinguishable subclasses—large-medium cells, small cells, cortisone-resistant cells, and dead cells.

Antigenic Subcylasses and Their Sedimentation Distribution: Cosedimentation

In order to analyze the sedimentation profile of BALB/c thymocytes according to surface Thy 1 concentration, 5×10^7 cells were incubated with anti-Thy 1.2 (and complement) diluted to a concentration which lyses about 50% (expt 1) or 80% (expt 2) of the cells, and the survivors were labeled with ^{51}Cr, mixed wth 2×10^8 untreated thymocytes and cosedimented as described. The cosedimentation profile for expt 2 is plotted in Fig. 8. There is a selective depletion in the smallest cell class (modal peak = fraction 37), with no detectable depletion in fractions

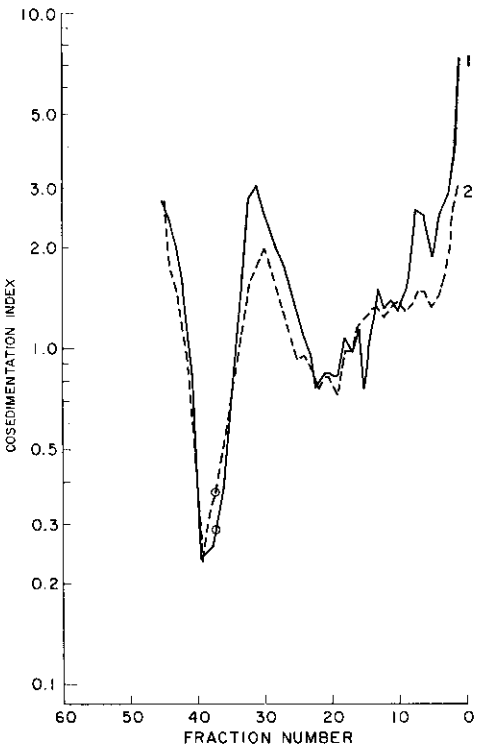

FIG. 6. Cosedimentation index profile of 5-day-old BALB/c donor CR thymocytes cosedimented with 5-day-old untreated BALB/c donor thymocytes.

corresponding to Pools B and C (Fig. 1a). A similar profile was obtained with C57BL TL+ thymocytes surviving treatment with congenic αTL antisera (Fig. 9). These data indicated that the major cell population in the thymus, the small lymphocytes, were relatively more sensitive to antisera plus C for both Thy 1.2 and

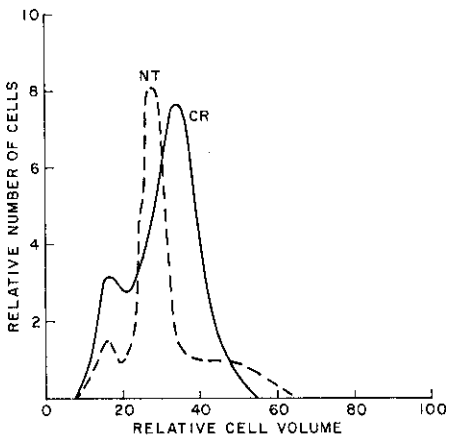

FIG. 7. Scatter frequency distribution for NT or CR thymocytes. Note that the relative size of CR thymocytes is intermediate between scatter peak 2 and 3 (Fig. 2a) yet is contained within pool B (Fig. 1b).

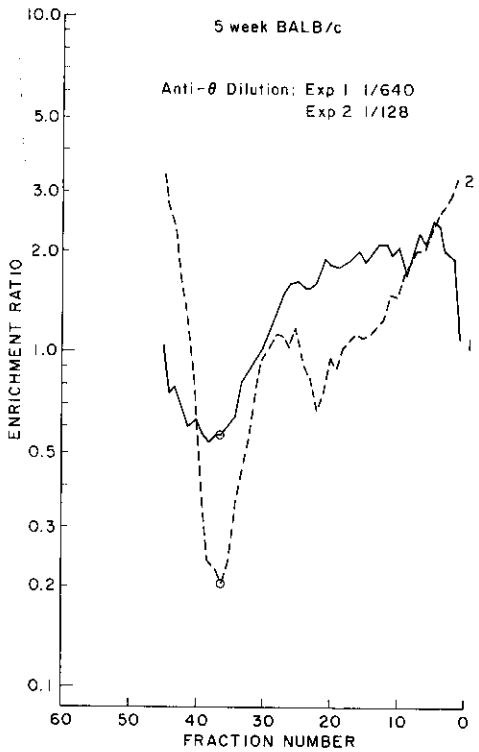

FIG. 8. Cosedimentation index profile of 2×10^7 ^{51}Cr-labeled BALB/c thymocyte survivors of αThy 1.2 treatment, cosedimented with 2×10^8 untreated thymocytes from the same donor. Experiment 1 used anti-Thy 1.2 at 1/640 dilution and ~ 50% of the cells were not lysed. Experiment 2 used anti-Thy 1.2 at 1/128 dilution, and ~ 20% of the cells were not lysed.

TL, as compared to pool C (large and medium) and pool B (CR-containing fraction) cells (see Fig. 1 for designation of pools).

Fluorescence Analysis of αThy 1.2-Stained BALB/c Thymocytes

When unfractionated NT cells are stained with fluoresceinated αThy 1.2, and then analyzed for fluorescence intensity excluding dead cells (Peak 1, Fig. 2a) from analysis by electronic gating (methods, 6), one obtains the distribution shown in Fig. 10. Three major peaks are seen, all with fluorescence above background (AKR/J thymocytes stained with fluoresceinated αThy 1.2 served as background controls for fluorescence). The dimmest peak corresponds with CR cells (which are shown superimposed in Fig. 10). If one selects (by electronic gating) the dimmest vs the two brighter fluorescence subpopulations and analyzes their scatter distributions, one obtains the distributions shown in Fig. 11. The dull cells distribute in scatter peaks coincident with CR with a proportion of dead cells. (When compared to Fig. 7, note the relative skewing of the scatter profile of CR thymocytes due to contaminant dead cells). The brighter cells distribute in scatter peaks 1, 2, and 3 (Fig. 2a). Fluoresence analysis of cells in 1*g* gradient fractions A, B, and C (Fig. 1b), after staining with fluoresceinated αThy 1.2, gives curves shown in Fig. 12 (the heights of the three peaks are not comparable but the relative fluorescence intensities are). Pool A, which consists of small thymocytes,

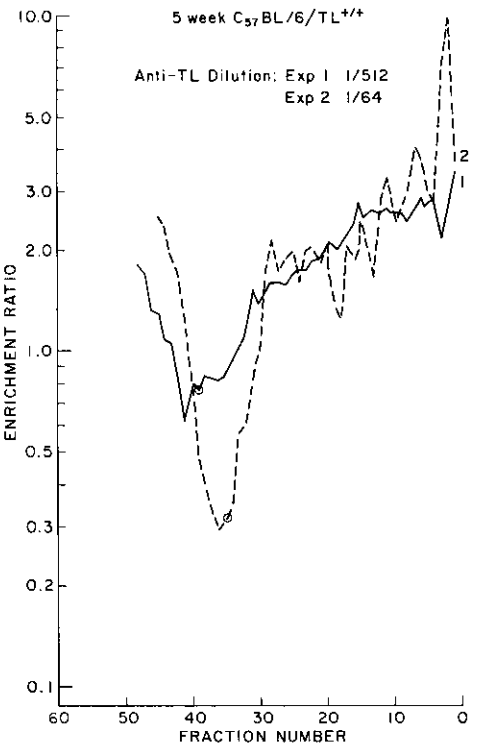

FIG. 9. Cosedimentation analysis of 2×10^7 ^{51}Cr-labeled C57BL/6TL+ thymocyte survivors of αTL treatment, cosedimented with 2×10^8 untreated thymocytes from the same donor. In expt 1, nearly 70% of the cells survived antiserum-mediated lysis, whereas in expt 2, only about 30% of the cells survived cytolysis.

coincides with the middle fluorescence peak in Fig. 10, while pool B (CR-enriched) contains mostly dim cells. The large and medium cells in pool C are mostly contained in the brightest fluorescence peak. By calculation, the modal fluorescence

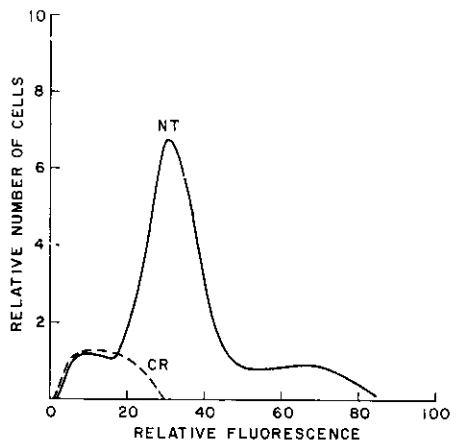

FIG. 10. Frequency distribution of fluorescence intensity of NT stained with anti-Thy 1.2 compared with a frequency distribution of the fluorescence intensity of CR thymocytes which has been superimposed. Note the correlation of CR fluorescence intensity with the dullest subpopulation of the total thymocyte fluorescence distribution.

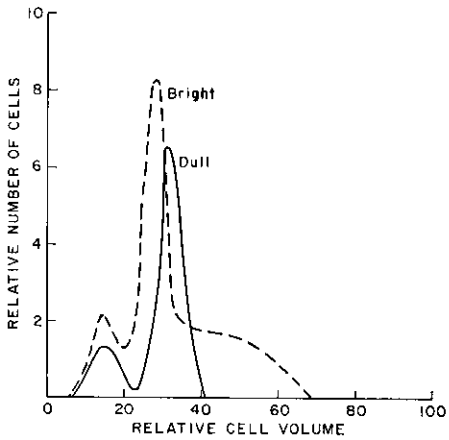

FIG. 11. Scatter frequency distribution of the fluorescence-dull subpopulation from Fig. 10 is compared to the relative cell volume of the remaining brighter subpopulations. Note the presence of dead cells within both subpopulations selected for fluorescence intensity.

per cell of pool C cells is approximately 1.3 × that of pool A, and 3.2 × that of the dim pool B cells. Calculating the surface area of these populations at their modal peaks, pool C cells have approximately 1.6 × the area of pool A cells, and 1.2 × the area of pool B cells; thus, the average Thy 1.2 density (detected by fluorescence) per unit area of pool A and pool C cells is similar, whereas most pool B cells express very little Thy 1.2 per unit area in comparison. (In fact, from these curves, the relative concentration of Thy. 1.2 per unit surface area [assuming a smooth sphere] for pool A cells is 1, pool B cells is 0.3, and pool C cells is 0.85.)

Absorption of Cytotoxic Anti-Thy 1.2 by Thymus Cell Subclasses

The data presented in Fig. 13 and 14 demonstrate the relative concentration of Thy 1.2 per cell as measured by absorption of cytotoxic anti-Thy 1.2 with graded

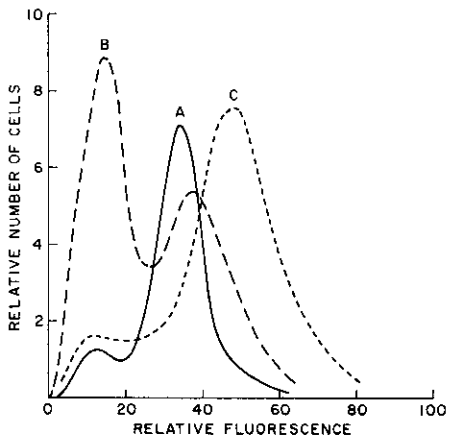

FIG. 12. Frequency distribution of fluorescence intensity of the pooled 1*g* cell populations (as displayed in Fig. 1b). Note the relatively large fraction of dull cells seen in pool B. These cells correspond in fluorescence intensity and in size to CR thymocytes. Note the relative depletion of dull cells from pools A and C. Again the ordinate portrays relative number of cells per fraction.

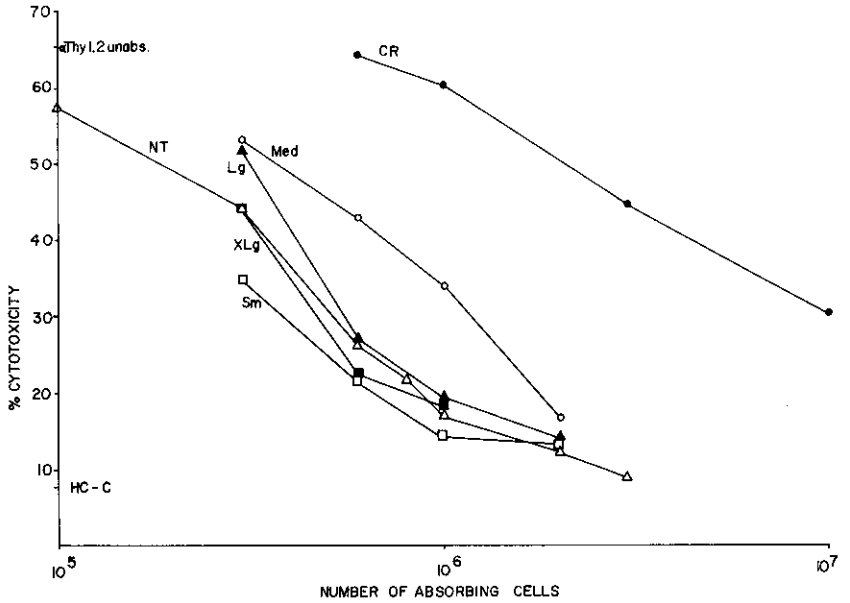

FIG. 13. Absorption of αThy 1.2 cytolytic activity by graded numbers of thymus cells of differing size or CR cells. αThy 1.2, at a final dilution of 1/100, was absorbed at 37° C with graded number of BALB/c thymocytes of each subclass for 45 min, and the absorbing cells removed by centrifugation. The supernatants were immediately tested (in duplicate) in a two-stage cytotoxic ^{51}Cr-release assay against unfractionated BALB/c thymocytes. The results are plotted as percentage of residual cytotoxicity vs log cell number used for absorption.

numbers of thymus cells of various subclasses. Figure 13 shows the cell-dose-dependent absorption of a single concentration of cytolytic αThy 1.2 (1:00), followed by testing against labeled, unfractionated thymocytes. For this experiment only, pool C cells were subfractionated into extra large and large cells. The absorption capacity per cell of these cells (pool C, large or extra large) was no greater than, and repeatedly (six experiments), somewhat less than small thymocytes (pool A). Pool B cells exhibit less absorption per cell than either pool A or pool C, but show significantly greater absorption than CR thymocytes, presumably reflecting their mixture of CR-like (~50%) and pool A and pool C cells (see Fig. 12). Similar cytotoxic absorption hierarchies are found using large thymus cells (pool C) or small cells (pool A) as targets. The direct cytotoxicity of unabsorbed αThy 1.2 at this dilution (1:100) in the presence of horse complement gives ~75% lysis of pool A cells, and only 44% lysis of pool C cells. This direct cytotoxic test may reflect the relative density of antigenic determinants on these cell subclasses, whereas cytotoxic absorption and relative fluorescence probably measure the total content of Thy 1.2 per cell. Figure 14 demonstrates the differential absorption capacity of CR as compared with NT cells in a different test. Anti-Thy 1.2 at 1:20 was absorbed with graded doses of CR or NT cells, and then titered in a cytotoxic assay against labeled NT cells. NT cells clearly absorb much more anti-Thy 1.2 than CR cells.

Subclass Maturation Pathways

In the foregoing sections we have defined at least four distinct and separable subclasses of BALB/c thymocytes: (1) dead or fragile cells; (2) small thymic lympho-

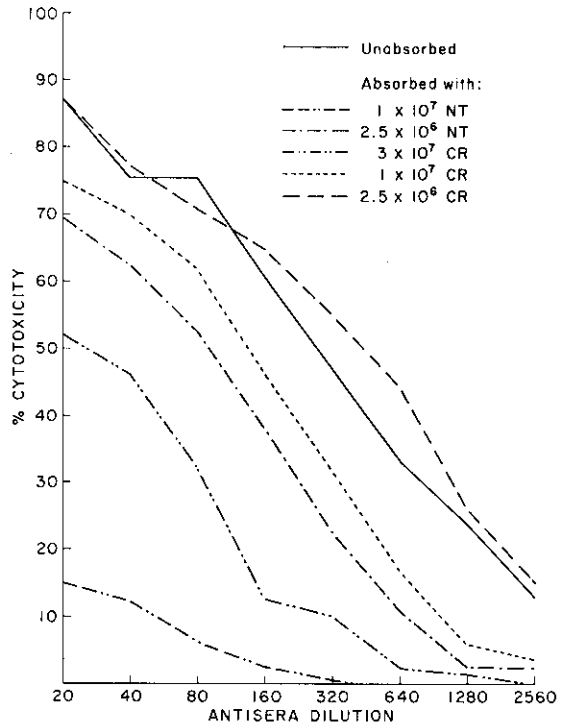

FIG. 14. Absorption of αThy 1.2 cytolytic activity by graded numbers of CR and NT cells. Anti-Thy 1.2 diluted to 1:20 final was absorbed as described in Fig. 13 with NT or CR cells, then tested in a two-stage cytotoxic ^{51}Cr-release assay in 2-fold dilutions against NT cells. The results are plotted as percentage of residual cytotoxicity vs antiserum dilution.

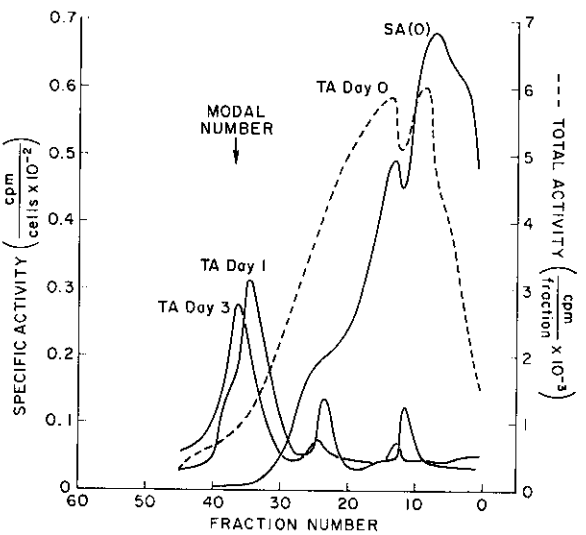

FIG. 15. Sedimentation analysis of *in situ* surface labeled 5-day-old donor BALB/c thymus cells as a function of time after topical labeling with ^{3}HTdR. The data are graphed as either total activity (TA = cpm/fraction) or specific activity (SA = cpm/100 cells). Every fraction was tested, but the data points are removed for clarity of presentation. (The graphs represent connections of all data points.) In all three experiments, the modal cell peak was at fraction 37. Two modes of TA were seen 1 hr after labeling (Day 0), at fractions 7 and 14. By day 1 the modal TA was at fraction 35, and by day 3, fraction 37.

cytes; (3) large and medium thymic lymphocytes; and (4) a class of thymocytes which share anti-Thy 1.2 fluorescence, scatter intensity, and sedimentation properties with CR thymocytes. It is the object of the following sections to analyze intersubclass maturation pathways, by selectively labeling *in vivo* a single subclass of cells.

Sedimentation Analysis of Surface-Labeled Neonatal Mouse Thymus

A previous observation had indicated that [^{3}H]thymidine applied to the surface of the thymus could be detected initially in cells of the outer cortex, and subsequently in cells of the deeper cortex and the medulla (1, 2). From autoradiographic sections it seemed that the earliest labeled cells were larger than the majority of thymocytes, and so an experiment was performed to determine which size cells were labeled by this procedure. [^{3}H]Thymidine (0.2–0.3 μCi/lobe) was applied topically to the ventral surface of the exposed thymus lobes of 4- to 5-day-old ice-anesthetized BALB/c hosts. Simultaneously, and each day thereafter, 0.02 ml of 1×10^{-2} *M* thymidine was injected intraperitoneally or subcutaneously to in-

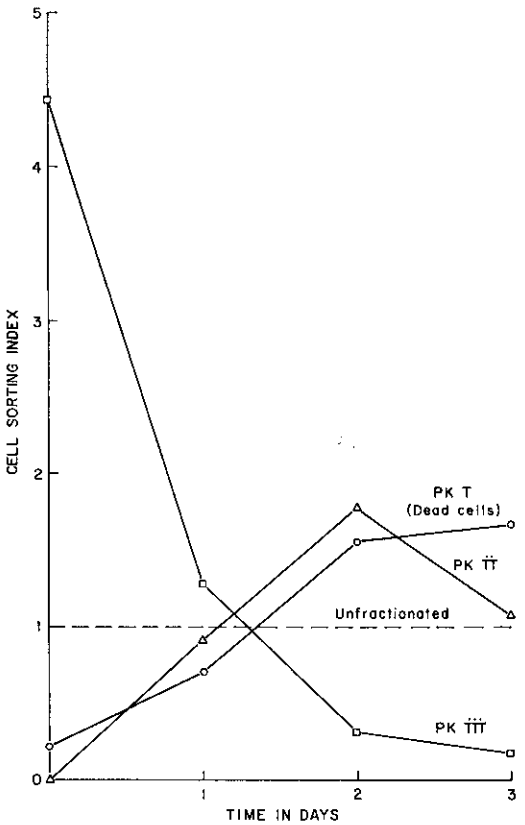

FIG. 16. A comparison of the appearance of label within different scatter-defined subpopulations as a function of time after labeling. The ratio of the labeling index of test cells to unfractionated cells is plotted on the ordinate, and labeling to sacrifice interval on the abcissa. Not only peak 3 (large) cells are labeled at time zero. There then follows a disappearance of label in peak 3 coincident with the appearance of label in peaks 1 and 2. Peaks 1 and 2 label in parallel.

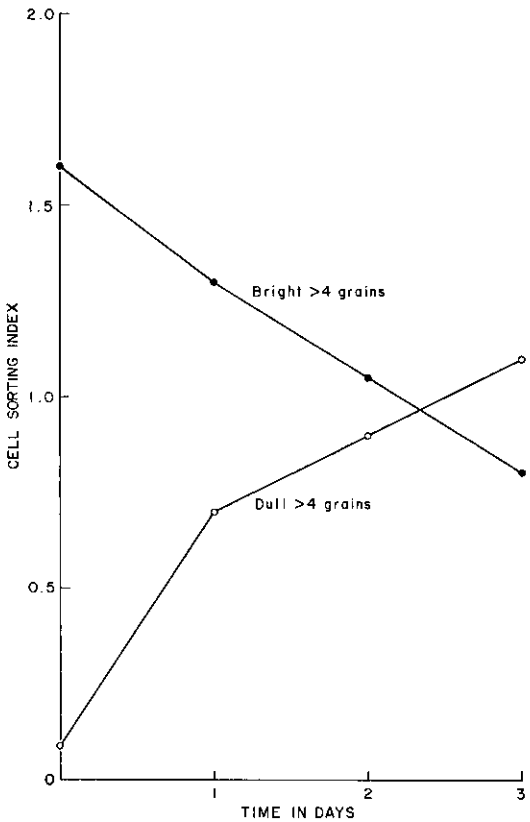

FIG. 17. The comparison of appearance of label in cells fractionated in the FACS by anti-Thy 1.2 fluorescence intensity over time. Only bright cells label at time zero and then the label appears in dull cells (CR) as it disappears from the bright fraction over 3 days.

hibit extrathymic [^{3}H]thymidine incorporation or reutilization of label from dying cells.

In Fig. 15 it can be seen that 1 hr after application of [^{3}H]thymidine to the surfaces of neonatal thymus, label is concentrated in pool C (i.e., larger cells). It is thus apparent that dividing lymphocytes of the subcapsular zone of the thymic cortex vary in size from the largest to the medium large. Since there are relatively few of these cells, the cpm per fraction shown corresponds to a considerable amount of [^{3}H]thymidine per cell. By 24 hr after administration of [^{3}H]thymidine, most of the label has shifted to the smaller cell fractions (pools A, B), with some residual counts in region C. After 48 or 72 hr, [^{3}H]thymidine is almost exclusively in the fractions of smaller thymocytes (pools A and B, Fig. 1a), suggesting that the cells initially labeled had divided or differentiated to progeny of smaller size. Although the small cell peak contains little or no label immediately after surface labeling, the fact that it contains most of the label by 24 hr indicates that the majority of DNA-synthesizing large cells are withn 1–3 generations (11, 12) of maturing to smaller cells. Furthermore, the fact that considerable label is retained in the small cell peak at 72 hr indicates that these cells have an intrathymic life-span (without dividing) of at least 2 days. Finally, the retention of label in region C in measurable amounts even up to 72 hr after topical labeling might be due to

asymmetric division of these larger cells, or entry of labeled cells into a noncycling state, or reversion of some small cell progeny to larger cells. The first possibility has been inferred from data presented by Bryant (11).

Sedimentation analysis of topically labeled thymocytes from adult hosts was also carried out at each time point, and gave results similar to those shown in Fig. 15. Since sedimentation analysis allows detection of label shifts between regions C and A most efficiently, but cannot accurately assess the label shifts from, or to cells bearing a low density of Thy 1.2 (CR-like) or dead cells, we performed several experiments on the maturation sequence as analyzed by fluorescence analysis.

Fluorescence and Scatter Analysis of Surface Labeled Neonatal BALB/c Thymus

The thymuses of 4- to 5-day-old BALB/c mice were labeled topically *in situ* as in the previous experimental section. At varying times thereafter, thymus cell suspensions were prepared, and sorted by scatter or fluorescence intensity. In the former, scatter peaks 1 (Fig. 2), 2 (Fig. 2, small cells), and 3 (Fig. 2, large and medium cells) were analyzed as to the relative percentage of labeled cells per subclass, and this was expressed as the scatter-labeling index (see Methods) (Fig. 16). The label is limited to cells in peak 3 30 min after application of ^{3}HTdR, and by 24 hr, the proportion of labeled cells is increasing in peaks 1 and 2, and decreasing in peak 3. High proportions of labeled cells are limited to peaks 1 and 2 by 48 and 72 hr after thymidine application. Since peak 1 represents dead cells, it is of interest that this peak contains rare (or no) labeled cells at 30 min, but increasing proportions of labeled cells at later times. It is evident that the dead cells do not become labeled until the appearance of label in the viable small cell population. This raises the interesting possibility that these cells have died *in vivo,* although selective fragility of small cells has not been ruled out in this study.

In the final set of separation experiments, we compared the labeling index of the anti-Thy 1.2 brightest (large and medium) and dimmest (CR-like) fractions at varying intervals after topical administration of ^{3}HTdR. The results are shown in Fig. 17. Dull cells are not labeled immediately after topical administration of ^{3}HTdR, whereas the brightest fractions are. With increase in time, the labeling index of dull cells increases, while the labeling index of bright cells decreases. Thus, dull cells also represent progeny of large, high Thy 1.2 (by fluorescence) cells.

DISCUSSION

Sedimentation, scatter, and fluorescence (with fluoresceinated anti-Thy 1.2) analysis of BALB/c thymocytes reveals several distinctive subclasses: (1) Dead (or fragile cells; (2) Small cells with intermediate Thy 1.2 fluorescence; (3) A broad peak of large cells which exhibit very bright Thy 1.2 fluorescence; and (4) Mid-size cells with low, but above-background Thy 1.2 fluorescence. Labeling of thymus outer cortical DNA synthetic cells by topical application of ^{3}HTdR *in situ* initially labels only subclass 3 of these cells. These large bright cells serve as progenitors for all three of the other subclasses during the 1–3 days after initial labeling. In a previous paper, utilizing the same labeling technique, cortisone-resistant medullary cells were shown to be derived from cortisone-sensitive outer cortical precursors (1). However, it was conceivable that the selective agent, hydrocortisone, affected the maturation sequence itself rather than simply deplet-

ing cortisone-sensitive subpopulations. Therefore, it was important to identify in untreated hosts an equivalent subpopulation of cells which are the product of maturation of outer cortical precursors. Cortisone-resistant cells share antigenic, sedimentation, and scatter properties with and are indistinguishable from subpopulation (4)—medium-sized lymphocytes with low Thy 1.2 fluorescence. Experiments in progress demonstrate that these cells share the properties of mitogen responsiveness (using PHA and ConA) with CR cells (V. Sato *et al.*, unpublished observations). Therefore, the fact that these cells are also, at least in part, the descendants of outer cortical dividing cells in untreated hosts confirms our earlier findings. It is likely that these cells are the low-density so-called Th_c or Th_{csr} cells described by several groups (13–16). It should be noted that pathways of maturation which derive from cells other than subpopulation (3) are not susceptible to this method of analysis, and, therefore, we may be missing other important maturation sequences. It also should be noted that this analysis did not reveal a difference in maturation time from subclass (3) to the other three subclasses. This brings up the important point that there is no evidence here presented that sequential maturation from subclass (3) must proceed through any subclass to any other subclass. Therefore, it is possible that the three "mature" subclasses could be descendants of either common or independent "immature" progenitor cells in the outer cortex. Furthermore, we do not know if subclass (1) represents cells that are dead *in situ*, and, therefore, represent a late event in thymus cell maturation, are selectively radiosensitive to the doses of incorporated ^3H (calculated to be less than 10 rads per cell), or are merely more susceptible than other subpopulations to possible damage in the preparation of thymus cell suspensions.

The technique of 1*g* sedimentation of prelabeled cells at varying label–sacrifice intervals allows a rough estimate of the average cell cycle time of dividing thymocytes. This had previously been tested by autoradiographic analysis by several investigators (11, 12). If the proliferation of thymus cells is essentially exponential, the proportion of ^3H counts in subclass (3), as compared to the other subclasses, should shift in a predictable fashion with time. For example, the cells undergoing their last intrathymic division prior to differentiation should contain a little more than half the incorporated ^3HTdR if there is no great difference in cell cycle time (Tc) and DNA synthetic times (Ts) between the various proliferating progenitors. After 1 Tc, therefore, approimately half the ^3H counts should shift to the "mature" subclasses, and half remain in the proliferating subclasses. After two Tc's, the ratio in counts of mature to proliferating cells should be nearly 3, and after three generations, nearly 7. In fact, at 24 hr, the ratio is approximately 4, implying that between two and three cycle times were completed, giving an average Tc of less than 12 and greater than 8 hr, which is in good agreement with autoradiographic analysis (11, 12). This calculation assumes that there is little cell loss during this interval. A more complete analysis of this technique would require examining the fine structure of label shift at times shorter than 24 hr.

The antigenic analysis of thymocyte subclass maturation sequence was limited in the paper to those subclasses defined by αThy 1.2 fluorescence intensity. Insofar as this is used to define the relationship between Cr-like and other thymocyte subclasses, this reflects accurately subclasses defined by absorption analysis (Figs. 13 and 14). However, it is not certain that fluorescence intensity and cytolytic efficiency of αThy 1.2 detects the same antigenic determinants, and, therefore

defines the same cell subclasses. Work in our laboratories (17, and I. Weissman, unpublished observations) indicates some interesting discordance between the two methods of assay in defining thymocyte and peripheral T cell subclasses, and, therefore, our conclusions on Thy 1.2 thymocyte subclass maturation pathways is limited to the fluorescence analysis. Quantitative fluorescence–size analyses and sorting with other cell surface antigens such as H-2 and Ly may help to understand further thymus maturation pathways and controls.

Note added in proof. Shortman and Jackson (18) have quite recently published data which they interpret as evidence for two *independent,* self-generating subclasses of thymocytes: A major population of high Thy 1.2 and a minor population of low Thy 1.2 cells. (The relative amount of Thy 1.2 per cell was inferred from the differential susceptibility to lysis of two cell populations by α-Thy 1.2 antisera at a high dilution with reduced concentrations of complement, and a shortened incubation time.)

They find that parenterally administered [^{3}H]TdR labels large cells of both antigenic subclasses and that label accumulates with time in small cells of both antigenic subclasses. They interpret their data as evidence that two independent maturational lineages exist, distinguished by surface Thy 1.2 expression. Unlike the experiments described in this paper, in their experiments label was not initially limited to a single subclass of cells within or without the thymus, and therefore they could not rule out a maturational lineage described here—high Thy 1.2 large cells → low Thy 1.2 midsize cells. As we have stated previously (1) and in this paper (see Discussion), we cannot rule out other subclass maturation pathways which involve dividing cells not in the thymic outer cortex. Indeed, Clark (19) has described a population of dividing cells in the thymic medulla, and we (I. L. Weissman, unpublished data) confirm that these cells are cortisone resistant *in vivo.* Thus, it is possible that self-generation of low Thy 1.2 cortisone-resistant thymocytes occurs *in addition* to the pathway described here.

A second possible explanation of the difference between the data reported here and by Shortman and Jackson lies in the different techniques for assessing the amount of Thy 1.2 per cell. As we have stated in the Discussion, large thymocytes have the most Thy 1.2 by fluorescence assay, but have less than small thymocytes by either direct cytotoxic (complement-dependent) testing or absorption of cytotoxic antisera. Thus, large thymocytes may appear to be low Thy 1.2 by cytotoxic assay (as carried out by Shortman and Jackson)—and therefore be similar to cortisone-resistant thymocytes—but differentiated from the cortisone-resistant subclass by fluorescence assay.

ACKNOWLEDGMENTS

Ms. Libuse Jerabek and Ms. Emi Kusaba provided excellent technical assistance, Ms. Lois Johnson provided excellent histological and autoradiographic preparations. We are indebted to George Gutman and David Korn for criticism of this manuscript. A portion of this work was presented to the FASEB intersociety Symposium on Development and Aging, April 7–12, 1974.

REFERENCES

1. Weissman, I. L., *J. Exp. Med.* **137**, 504, 1973.
2. Bryant, B. J., *In* "Morphological and Fundamental Aspects of Immunity" (K. Lindahl-Kiessling, G. Alm, and M. Hanna, Eds.), pp. 103–112. Plenum, New York, 1971.
3. Miller, R. G., and Phillips, R. A., *J. Cell Physiol.* **73**, 191, 1969.
4. Rosenberg, S. A., Levy, R., Schechter, B., Ficker, S., and Terry, W. D., *Transplantation* **13**, 541, 1972.
5. Weissman, I. L., *J .Exp. Med.* **126**, 291, 1967.
6. Hulett, H. R., Bonner, W. A., Sweet, R. G., and Herzenberg, L. A., *Clin. Chem.* **19**, 813, 1973.
7. Julius, M. H., Sweet, R. G., Fathman, C. G., and Herzenberg, L. A., Los Alamos, N. M., AEC Symposium Series (C.O.N.S. 73–1007), Oct. 17–19, 1973.
8. Cebra, J. J., and Goldstein, G., *J. Immunol.* **95**, 230, 1965.

9. Rotman, B., Papermaster, B. W., *Proc. Nat. Acad. Sci. USA* **55**, 134–141, 1966.
10. Westring, D. W., and Brittin, S. B., *Cytobios* **2**, 117, 1969.
11. Bryant, B. J., *Eur. J. Immunol.* **2**, 38, 1972.
12. Metcalf, D., and Wiadrowski, M., *Cancer Res.* **27**, 483, 1966.
13. Konda, S., Nakao, Y., and Smith, R. T., *J. Exp. Med.* **136**, 1461, 1972.
14. Levey, R. H., and Burleson, R., *Cell Immunol.* **4**, 316, 1972.
15. Cohen, J. J., Fishbach, M., and Claman, H. N., *J. Immunol.* **105**, 1146, 1970.
16. Blomgren, H., and Andersson, B., *Cell. Immunol.* **1**, 545, 1970.
17. Cantor, H., Simpson, E., Sato, V. L., Fathman, C. G., and Herzenberg, L. A. Submitted for publication, 1974.
18. Shortman, K., and Jackson, H. *Cell. Immunol.* **12**, 230, 1974.
19. Clark, S. L., Jr., *J. Exp. Med.* **128**, 927, 1968.